

## Dust Cavities around White Dwarfs

### WD0038+730 and WD0531-022

**Bhanu Bhakta Sapkota**

Central Department of Physics  
Tribhuvan University, Kirtipur, Nepal

**Ronald Weinberger**

Institute of Astroparticle Physics  
Innsbruck University, Technistrasse 25/8, Innsbruck, Austria

**Binil Aryal**

Institute of Science & Technology  
Tribhuvan University, Kirtipur, Nepal

This article is distributed under the Creative Commons by-nc-nd Attribution License.  
Copyright © 2021 Hikari Ltd.

#### Abstract

We present dust color temperature, dust mass and Planck function distributions in the two far infrared cavities located within  $0.25^\circ$  of white dwarfs WD0038+730 and WD0531-022. For this, IRAS (Infrared Astronomical Satellite) data at longer wavelengths (60 and 100  $\mu\text{m}$ ) have been used. The dust color temperature is found to lie in the range 19.5-30.3 ( $\pm 2.6$ ) K. In both cavities, the period of oscillation is found to be 2-16 times larger than that of the amplitude of the oscillation. This suggests that the dust oscillates vigorously along the direction of white dwarf. Therefore, we noticed a significant influence of the wind emitted from the white dwarf in the process of formation and evolution of the far infrared cavity.

**Keywords:** White Dwarf, Far Infrared, Interstellar Dust, Dust color temperature, Dust mass, Planck function, Gaussian distribution, Dust oscillation

## 1 Introduction

Dust in the interstellar medium preserve signature of past evolutionary stages during late stage of the stellar evolution. In this context, central region of the planetary nebula is important not only because of electron degenerate processes at the core, but also asymptotically emitting wind at the surface. Because of the excessively high density and asymptotic burning of fuels (Hydrogen and Helium) at the central region, it creates a strong wind at the envelope [12]. These winds interact with ambient interstellar medium. In the Milky Way, there are more than 3000 such systems [14]. These systems strongly interact with the ambient interstellar medium. Our aim is to find out regions in which both dust and the central star (actually white dwarf) interact. This interaction might be due to the wind [18] or radiation and cosmic particles [6] or gravitational waves[22].

In this work, we aim to investigate far infrared cavities nearby white dwarfs (WDs hereafter) at 100  $\mu\text{m}$  IRAS (Infrared Astronomical Satellite, hereafter IRAS) [13] (<http://skyview.gsfc.nasa.gov>) maps surrounded by dust and study their physical properties such as dust color temperature, dust mass, Planck function and their distributions. Finally, we intend to understand relation between the possible dust oscillations towards the WD.

## 2 Region of Interest and Methods

We have carried out a systematic search at 100 and 60  $\mu\text{m}$  wavelengths of IRAS maps using a catalog of WDs compiled by Holberg et al. [14]. We are interested to find cavity candidates having a very low flux density at least 5 times lower than that of its background, assuming it has formed because of the wind emitted from the nearby WDs and its progenitors in the process of their evolution. Our selection criteria are as follows: (a) WD should be located within  $0.25^\circ$  of the cavity, (b) major diameter of the cavity should be at least  $0.25^\circ$  and (c) IRAS map should be available at both 100 and 60  $\mu\text{m}$  wavelengths. We noticed two such cavities around the WDs namely WD0038+730 and WD0531-022 (see Figs. 1a & 2a).

We have downloaded FITS (Flexible Image Transport System) image and used ALADIN2.5 software in order to find out values of flux densities at 100 and 60  $\mu\text{m}$  wavelengths. These values are corrected for both background and foreground emissions [19] and used to calculate dust color temperature ( $T_d$ ), dust mass ( $M_d$ ) and the Planck function ( $B(\nu, T)$ ) for each pixel using the formula given by [24, 21, 16, 1, 2],

$$T_d = -96 \frac{1}{\ln\{R \times 0.6^{(3+\beta)}\}} \quad (1)$$

$$M_d = 0.40 \left[ \frac{F_\nu D^2}{B(\nu, T)} \right] \quad (2)$$

$$B(\nu, T) = \frac{2h\nu^3}{c^2} \left[ \frac{1}{e^{\frac{h\nu}{kT}} - 1} \right] \quad (3)$$

Here  $R$  is the ratios of flux densities at 60 and 100  $\mu\text{m}$  and  $\beta$  represents spectral index of the cavity region. Spectral index depends upon the as composition of material (e.g, dust/grain constitute carbon and silicon compounds), its size, and compactness. Since the far infrared cavity is surrounded by dust and grains, the values of spectral index has been taken as 2 ( $\beta = 0, 1, 2$  for perfect black body, amorphous matter, metallic crystalline, respectively) [16]. In equation (2),  $F_\nu$  and  $D$  represent flux density at 100  $\mu\text{m}$  and distance to the cavity. The distance has been taken from the catalog [20]. The Planck function ( $B(\nu, T)$ ) is calculated for each pixel using its dust color temperature at 100  $\mu\text{m}$  wavelength.

### 3 Result & Discussion

At first, we introduce the white dwarf WD0038+730 by giving its properties. Second, we present far infrared cavity nearby WD observed at 60  $\mu\text{m}$  and 100  $\mu\text{m}$  IRAS images. We have calculated dust color temperature; dust mass and hence Planck function distributions using expressions (1-3).

#### 3.1 Far infrared cavity nearby white dwarf WD0038+730

The white dwarf WD0038+730 is located at R.A. (J2000) =  $00^{\text{h}}41^{\text{m}}46.1^{\text{s}}$ , Dec. (J2000) =  $+73^{\circ}21'10''$ . This white dwarf belongs to the spectral class DQ5C [15]. DQ classification refers to the carbon features, either atomic or molecular, in any part of the electromagnetic spectrum. The spectra of this WD do not show Balmer or ionized Helium lines [9]. Therefore, this WD cannot be observed through optical telescope. The parallax and proper motion of the WD are 0.0468 mas and 0.071 (RA), 0.067 (Dec.)  $\text{mas yr}^{-1}$  respectively [7]. Therefore WD0038+730 is relatively old and cool.

Figure 1(a) shows 100  $\mu\text{m}$  IRAS Joint Photographic Experts Group (JPEG) image of  $0.3^\circ \times 0.3^\circ$  field in which a cavity (symbol 'X') can be seen along with the WD0038+730 (symbol '+'). A huge extended infrared emission at longer wavelength can be seen at the north-east of the field (Fig. 1b). The size of cavity is  $14.10' \times 6.40'$ . The distance between WD and center of cavity (the region of flux minima) is  $16.60'$ . We focus our study at the central part of the field, shown in the image. The maximum flux outside the cavity is found to be in the range  $18.98 - 5.29 \times 10^9 \text{ MJy sr}^{-1}$ . In the image, the black and red color represents the minimum and maximum flux density. There are 43 pixels in the cavity. We have measured flux densities at both 100  $\mu\text{m}$  and 60  $\mu\text{m}$  FITS images using ALADIN 2.5 software and calculated dust color temperature, dust mass and Planck function of each 43 pixels using equations (1-3).

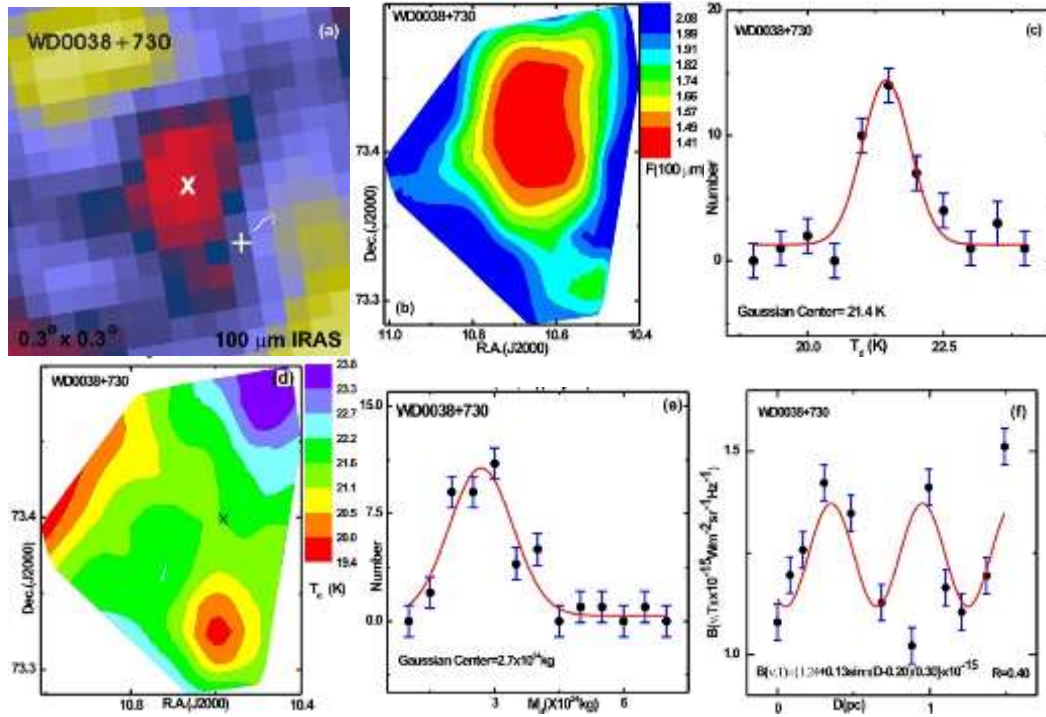


**Figure 1:** (a)  $0.3^\circ \times 0.3^\circ$  field of far infrared cavity nearby white dwarf WD0038+730 centered at R.A. (J2000) =  $00^h41^m43^s$ , Dec (J2000) =  $+73^\circ21'14''$ . The position of the WD (symbol '+') and center of cavity (symbol 'x') are shown. (b) Flux density contour map at  $100 \mu\text{m}$ . The distribution of dust color temperature (c,d), dust mass (e) and Planck function (f) are shown. The solid curve represents Gaussian (c,e) and sinusoidal (f) fits. The Gaussian parameters and the contour levels are shown. The statistical  $\pm 1\sigma$  error bars are shown.

Figure 1(c) shows the distribution of dust color temperature in the region of interest. The minimum and maximum dust color temperatures are found to be  $19.5 \pm 1.2 \text{ K}$  and  $23.8 \pm 2.6 \text{ K}$ . Gaussian fit is shown by the solid line. The Gaussian function is

$$y = y_0 + \frac{Ae^{-\frac{4\ln 2(x-x_c)^2}{\omega^2}}}{\omega \sqrt{\frac{\pi}{4\ln 2}}} \quad (4)$$

Where  $y_0$ ,  $A$ ,  $x$  and  $x_c$  represent Gaussian offset, area width, and center, respectively. After substituting the values of Gaussian parameters from the Figure 1(c), number distribution of dust color in the cavity is found to be,

$$n_T = 1.3 + 15.02e^{-3.42(T_d-21.4)^2} \quad (5)$$

Similarly, number density distribution of dust mass in the cavity (Figure 1e) is

$$n_M = 0.39 + 11.90e^{-1.30 \times 10^{-48}(M_d-2.78 \times 10^{24})^2} \quad (6)$$

In the far infrared cavity, both dust color temperature and dust mass show Gaussian like distribution. It suggests that the cavity nearby WD0038+730 is stable and possibly formed long ago because the nearby white dwarf is also aged. The southern part of the cavity is the coolest region. The density of low temperature region should be high enough. The low temperature region is found to be massive, obeying linear relationship between mass and density at constant volume. It means cosmological principle (homogenous and isotropic) is assumed to be valid.

The dust particles obey Maxwellian velocity distribution and the radiation coming to it follows Planck's theory. It is expected that the dust-radiation to follow local thermodynamic equilibrium. For this distribution of Planck function should be uniform. Figure 1(f) shows the distribution of Planck function from the WD towards the center of the cavity. Planck function is found to be deviated from the straight line. We have fitted the distribution considering dust oscillation. The parameters namely offset, amplitude, period, and phase shift are determining factors whether the region is in the strong dynamical equilibrium or not. The sinusoidal function is

$$y = y_0 + A \sin \frac{\pi(x-x_c)}{\omega} \quad (7)$$

where  $y_0$ ,  $A$ ,  $x_c$ , and  $\omega$  represent offset, amplitude, phase shift, and period respectively. We get distribution as

$$B(\nu, T) = 1.24 + 0.13 \sin \left[ \frac{\pi(D-0.20)}{0.30} \right] \times 10^{-15} \quad (8)$$

Here the period of oscillation is found to be two times larger than the amplitude. It suggests the dust oscillation towards the WD.

To sum up, the white dwarf WD0038+730 is found to affect nearby region in the process of evolution. Due to this, an infrared cavity has been formed.

### 3.2 Far infrared cavity nearby white dwarf WD0531-022

White dwarf WD0531-022 is centrally located in the far infrared dust cavity at R.A. (J2000) = 05<sup>h</sup>34<sup>m</sup>20<sup>s</sup>, Dec. (J2000) = -02°14'32". The spectral class of this WD is DA [11] having Balmer lines in the spectra [9]. Its spectra do not have neutral Helium or any metallic lines. Therefore the surface temperature of this WD is hot. The parallax of this white dwarf is 0.0904 mas and its proper motion is 0.140 mas yr<sup>-1</sup> (RA), 0.129 mas yr<sup>-1</sup> (Dec.) [7]. The WD is moving towards north-east direction, as indicated by arrow in the Figure 2(a). The size of cavity is 20.1' x 7.8'. The distance between white dwarf and center of cavity is 3.23' and the cavity is located towards north of WD.

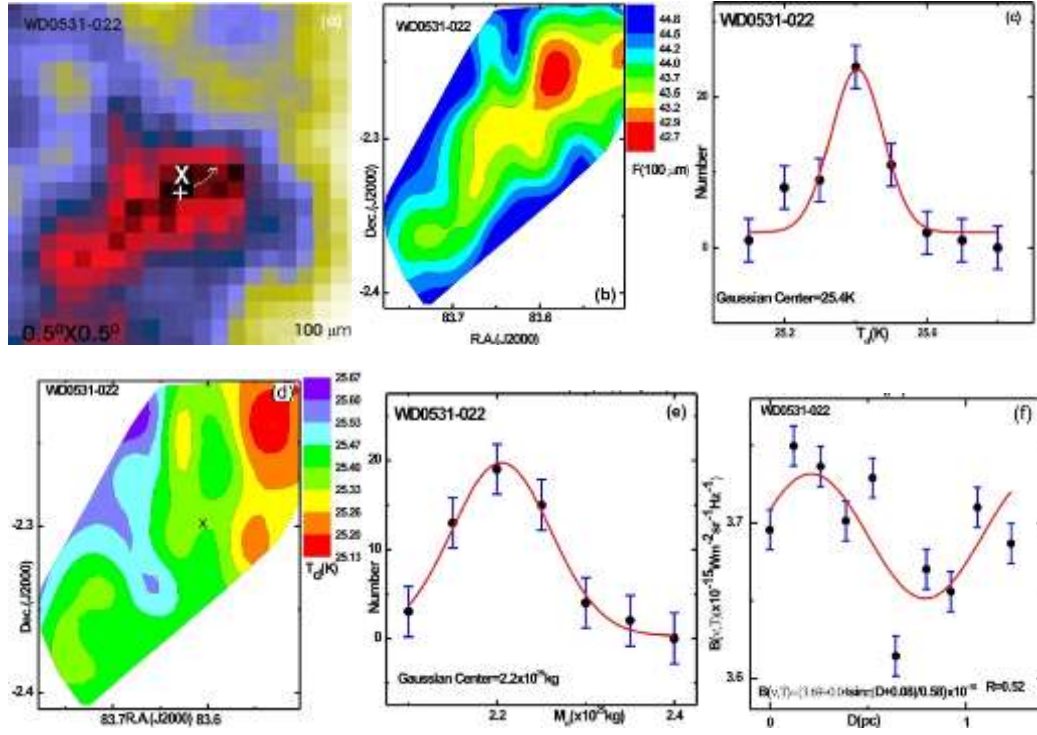


**Figure 2:** (a)  $0.5^\circ \times 0.5^\circ$  field of far infrared cavity nearby white dwarf WD0531-022 centered at R.A.(J2000)= $05^h34^m20^s$ , Dec (J2000) =  $-02^\circ14'32''$ . The position of white dwarf (symbol '+') and center of the cavity (symbol 'x') are shown. (b) Flux density contour map at  $100 \mu\text{m}$ . The distribution of dust color temperature (c,d), dust mass (e) and Planck function (f) are shown. The solid curve represents Gaussian (c,e) and sinusoidal (f) fits. The Gaussian parameters and the contour levels are shown.

There are 56 pixels in the cavity. Pixel size in IRAS  $100 \mu\text{m}$  map is  $1.52'' \times 1.52''$ . We worked on each pixel to find the values of flux densities at both 60 and  $100 \mu\text{m}$  IRAS images using ALADIN2.5 software. To calculate dust color temperature of each pixel, we used equation (1). The minimum and maximum dust color temperatures are found to be  $25.2 \pm 0.7 \text{ K}$  and  $25.7 \pm 0.5 \text{ K}$  respectively. Figure 2(b) showed contour map of flux density at  $100 \mu\text{m}$ . We have fitted the distribution of dust color temperature in the cavity using Gaussian (Fig. 1c). Similar to the above, distribution takes this form

$$n_T = 2.0 + 26.95e^{-142.86(T_d - 25.4)^2} \quad (9)$$

Dust mass distribution is found to have a positive skewness (Fig. 2d). The Gaussian distribution is

$$n_M = 0.30 + 23.16e^{-2.31 \times 10^{-48}(M_d - 2.20 \times 10^{25})^2} \quad (10)$$

Figure 2(f) shows sinusoidal fitting of the plot between Planck function along the distance between the WD and the flux minima of the cavity. The Planck function distribution is found to be,

$$B(\nu, T) = 3.69 + 0.04 \sin \left[ \frac{\pi(D-0.08)}{0.58} \right] \times 10^{-15} \quad (11)$$

Here the period of oscillation ( $\omega$ ) is found to be 16 times ( $0.58/0.04 \sim 16$ ) higher than that of the amplitude of the oscillation. Therefore, dust in this cavity oscillates vigorously towards the WD. This is obviously because of the wind emitted from the WD.

### 3.3 Comparison with other works

Low et al. [10] determined the temperature of cirrus cloud using 60  $\mu\text{m}$  and 100  $\mu\text{m}$  fluxes and found 21-27 K. Wood et al. [8] found 20-25 K temperatures of cirrus cloud. In our calculation, the dust color temperature of both cavities ranges from 19-31 K to which are nearly similar results obtained to that of [10] and Wood et al. [8]. Reach et al. [23] observed the white dwarf G29-38 using photometer and spectrograph of the Spitzer Space Telescope. They found a cloud of small grains about  $1-10R_{\text{sun}}$  far from G29-38 emitting in the mid infrared. The luminosity of the infrared excess is observed to be only 3% of the total luminosity of the star. Dong et al. (2010) identified a dust ring around the white dwarf WD2226-210 at the center of the Helix nebula. They concluded that the hot WD provides an intense source of UV radiation. Aryal et al. [4] studied Planetary nebula NGC 1514 on 12, 25, 60, and 100  $\mu\text{m}$  of the IRAS maps. They detected a huge (2.6 pc) dust emission region around the evolved planetary nebula NGC 1514 on 12 mm maps. Again they found two giant (2.1 and 0.9 pc) bipolar dust emission structures centered on planetary nebula NGC 1514.

Aryal & Weinberger [5] studied the dust structures in 100  $\mu\text{m}$  IRAS maps around white dwarf WD1003-44. They determined the dust color temperature in the range ( $20.7 \pm 0.6$ ) K to ( $21.6 \pm 0.2$ ) K, similar to the values that we have found. Jha et al. [2] measured dust color temperature of four far infrared loops G007+18, G143+07, G214-01 and G323-02 which are situated within  $1^\circ$  of pulsars namely PSR J1720-1633, PSR J0406+6138, PSR J0652-0142 and PSR J1535-5848 showed minimum and maximum temperatures from ( $19.4 \pm 1.2$ ) K to ( $25.3 \pm 1.7$ ) K. Gautam & Aryal (2019) estimated dust color temperature in four far infrared cavities nearby AGB stars namely, FIC01+55, FIC05+28, FIC06-05 and FIC06-01 and found minimum ( $18.3 \pm 1.2$ ) K and maximum ( $20.5 \pm 1.3$ ) K dust color temperatures.

## 4 Conclusion

We have investigated two cavities surrounded by the dust in IRAS maps at 60 and 100  $\mu\text{m}$  wavelengths. These far infrared cavities are found to be located nearby (within  $0.25^\circ$ ) white dwarfs WD0038+730 and WD0531-022. We have studied dust color temperature and dust mass distributions in the cavity. In addition, distribution of Planck function has been studied along the direction of neighboring white dwarfs. Our conclusions are as follows:

- (1) Far infrared cavity (size  $\sim 14.1'$  x  $6.4'$ ) located nearby white dwarf WD0038+730 showed maximum dust color temperature as  $23.8 \pm 1.6$  K and the minimum  $19.5 \pm 1.2$  K. The total mass of the dust is found to be  $1.3 \times 10^{26}$  kg. The distribution of Planck's function is found to be sinusoidal, with amplitude smaller by 2-fold than that of period of oscillation.
- (2) Far infrared cavity (size  $\sim 20.1'$  x  $7.8'$ ) located nearby white dwarf WD0531-022 showed maximum and minimum dust color temperatures  $30.3 \pm 2.6$  K and  $25.2 \pm 0.7$  K, respectively. We noticed that this cavity is 10 times massive than that of the first one. Similarly, period of oscillation is found to be 16 times more than that of the amplitude in the Planck function distribution.

Therefore, it is found that both cavities are formed and driven by the nearby white dwarfs. It would be interesting to work on the association of dust cavities and the white dwarfs in the future.

**Acknowledgements.** One of the authors (BBS) acknowledges University Grants Commission, Central Department of Physics, Mahendra Multiple Campus, Tribhuvan University, Nepal for various kinds of support during Ph.D. work. We are thankful to Dr. Ajay Kumar Jha, Ms. Namuna Adhikari and Mr. Ishwar Joshi for their help during data processing. We have used SkyView virtual observatory (<http://skyview.gsfc.nasa.gov>), SIMBAD (<http://simbad.u-strasbg.fr/simbad/>) for providing database and software ALADIN 2.5 (<https://aladin.u-strasbg.fr/>).

## References

- [1] A. Gautam and B. Aryal, A study of four low-latitude ( $|l| < 10^\circ$ ) far-infrared cavities, *Journal of Astrophysics and Astronomy*, **40** (2019), no. 2, 16-21. <https://doi.org/10.1007/s12036-019-9578-1>
- [2] A. Jha, B. Aryal and R. Weinberger, A study of dust color temperature and dust mass distributions of four far infrared loops. *Revista Mexicana de Astronomia Astrofisica*, **53** (2017), no. 2, 1-10. <http://www.scielo.org.mx/pdf/rmaa/v53n2/0185-1101-rmaa-53-02-00019.pdf>
- [3] A. Jha and B. Aryal, Dust color temperature distribution of two FIR cavities at IRIS and AKARI maps, *Journal of Astrophysics and Astronomy*, **39** (2018), no. 2, 24-34. <https://doi.org/10.1007/s12036-018-9517-6>
- [4] B. Aryal, C. Rajbahak and R. Weinberger, A giant dusty bipolar structure around the planetary nebula NGC 1514, *Monthly Notices of the Royal Astronomical Society*, **402** (2010), no. 2, 1307-1312. <https://doi.org/10.1111/j.1365-2966.2009.15966.x>

- [5] B. Aryal and R. Weinberger, Dust structure around white dwarf WD 1003-44 in 60 & 100 mm Iras survey, *Himalayan Physics*, **2** (2011), 5-10.  
<https://doi.org/10.3126/hj.v2i2.5202>
- [6] B. Aryal and R. Weinberger, A new large high latitude cone-like far-IR nebula, *Astronomy and Astrophysics*, **448** (2006) 213-219.  
<https://doi.org/10.1051/0004-6361:20042440>
- [7] C. Gaia, A. Brown, A. Vallenari, T. Prusti, J. de Bruijne, C. Babusiaux, et al., Gaia data release 2 summary of the contents and survey properties, *Astronomy & Astrophysics*, **616** (2018), no. 1, 1-10.  
<https://doi.org/10.1051/0004-6361/201833051>
- [8] D.O. Wood, P.C. Myers and D.A. Daugherty, Iras images of nearby dark clouds, *The Astrophysical Journal Supplement Series*, **95** (1994), 457-501.  
<https://doi.org/10.1086/192107>
- [9] E.M. Sion, J.L. Greenstein, J.D. Landstreet, J. Liebert, H.L. Shipman and G. Wegner, A proposed new white dwarf spectral classification system, *The Astrophysical Journal*, **269** (1983), 253-257.  
<https://doi.org/10.1086/161036>
- [10] F. Low, D. Beintema, T. Gautier, F. Gillett, C. Beichman, G. Neugebauer, Infrared cirrus-new components of the extended infrared emission, *The Astrophysical Journal*, **278** (1984), L19-L22. <https://doi.org/10.1086/184213>
- [11] G.P. McCook and E.M. Sion, A catalog of spectroscopically identified white dwarfs, *The Astrophysical Journal Supplement Series*, **121** (1999), no. 1, 1-20. <https://doi.org/10.1086/313186>
- [12] H. Karttunen, P. Kroeger, H. Oja, M. Poutanen, and K.J. Donner, *Fundamental Astronomy*, Springer, 2007.  
<https://doi.org/10.1007/978-3-540-34144-4>
- [13] IRAS Official Webpage <https://irsa.ipac.caltech.edu/IRASdocs/iras.html>
- [14] J.B. Holberg, Terry D. Oswalt and E.M. Sion, A determination of the local density of white dwarf stars, *Astrophysical Journal*, **571** (2002), 512-518.  
<https://doi.org/10.1086/339842>
- [15] J.L. Greenstein and J.W. Liebert, Spectrophotometry of white dwarfs as observed at high signal-to-noise ratio, *The Astrophysical Journal*, **360** (1990), 662-684. <https://doi.org/10.1086/169153>

- [16] K. Young, T. Phillips and G. Knapp, Circumstellar shells resolved in IRAS survey data. II-analysis, *The Astrophysical Journal*, **409** (1993), 725-738.  
<https://doi.org/10.1086/172702>
- [17] R. Dong, Y. Wang, D. Lin and X.W. Liu, Dusty disks around white dwarfs I, origin of debris disks, *The Astrophysical Journal*, **715** (2010), no. 2, 1036-1046. <https://doi.org/10.1088/0004-637x/715/2/1036>
- [18] R. Weaver, R. McCray, J. Castor, P. Shapiro and R. Moor, Interstellar bubbles. II - structure and evolution, *Astrophysical Journal*, **218** (1977), 377-395. <https://doi.org/10.1086/155692>
- [19] R. Weinberger and B. Armsdorfer, A pair of gigantic bipolar dust jets close to the solar system, *Astronomy and Astrophysics*, **416** (2004), L27-L30.  
<https://doi.org/10.1051/0004-6361:20040054>
- [20] S.J. Kleinman, S.O. Kepler, D. Koester, Ingrid Pelisoli, V. Pecanha, A. Nitta, J.E.S. Costa, et al., SDSS DR7 White Dwarf Catalog, *The Astrophysical Journal Supp. Ser.*, **204** (2013), no. 1, 1-14.  
<https://doi.org/10.1088/0067-0049/204/1/5>
- [21] S.L. Schnee, N.A. Ridge, A.A. Goodman and J.G. Li, A complete look at the use of IRAS emission maps to estimate extinction and dust temperature, *The Astrophysical Journal*, **634** (2005), no. 1, 442-450.  
<https://doi.org/10.1086/491729>
- [22] T. Padmanabhan, *An Invitation to Astrophysics*, World Scientific Series in Astronomy and Astrophysics: Volume 8, 2006.  
<https://doi.org/10.1142/6010>
- [23] W.T. Reach, M.J. Kuchner, T. Von Hippel, A. Burrows, F. Mullally, M. Kilic and D. Winget, The dust cloud around the white dwarf G29-38, *The Astrophysical Journal*, **635** (2005), no. 2, L161-L165.  
<https://doi.org/10.1086/499561>
- [24] X. Dupac, J.P. Bernard, N. Boudet, M. Giard, J M. Lamarre, C. Meny, et al., Inverse temperature dependence of the dust submillimeter spectral index, *Astronomy & Astrophysics*, **404** (2003), no. 1, L11-L15.  
<https://doi.org/10.1051/0004-6361:20030575>

**Received: October 9, 2021; Published: October 27, 2021**